Published online November 4, 2004

Nucleic Acids Research, 2004, Vol. 32, No. 19 ***5907–5915***
doi:10.1093/nar/gkh920

Centromere *parC* of plasmid R1 is curved

Christian Hoischen, Alexander Bolshoy[1], Kenn Gerdes[2] and Stephan Diekmann*

Institute for Molecular Biotechnology e.V., Beutenbergstr. 11, D-07745 Jena, Germany, [1]Institute of Evolution, University of Haifa, Haifa 31905, Israel and [2]Department of Biochemistry and Molecular Biology, University of Southern Denmark, Campusvej 55, DK-5230 Odense M, Denmark

Received August 18, 2004; Revised and Accepted October 14, 2004

ABSTRACT

The centromere sequence *parC* of *Escherichia coli* low-copy-number plasmid R1 consists of two sets of 11 bp iterated sequences. Here we analysed the intrinsic sequence-directed curvature of *parC* by its migration anomaly in polyacrylamide gels. The 159 bp long *parC* is strongly curved with anomaly values (*k*-factors) close to 2. The properties of the *parC* curvature agree with those of other curved DNA sequences. *parC* contains two regions of 5-fold repeated iterons separated by 39 bp. We modified 4 bp within this intermediate sequence so that we could analyse the two 5-fold repeated regions independently. The analysis shows that the two repeat regions are not independently curved parts of *parC* but that the overall curvature is a property of the whole fragment. Since the centromere sequence of an *E.coli* plasmid as well as eukaryotic centromere sequences show DNA curvature, we speculate that curvature might be a general property of centromeres.

INTRODUCTION

Stable maintenance of bacterial low-copy-number plasmids is ensured by a number of active stabilization loci encoded by the plasmids themselves. These loci can be divided into those that function by the killing of plasmid-free segregants [reviewed in (1,2)] and those that actively segregate plasmid copies to daughter cells at cell division, i.e. partitioning loci (*par*). All known plasmid *par* systems operate by determining the intracellular position of their replicon such that, after replication, plasmid copies are rapidly transported to each side of the bacterial septal plane where they remain positioned until cell division takes place. Thus, by actively distributing plasmid molecules to cell progeny, the *par* systems ensure faithful plasmid inheritance throughout the bacterial population (3–6). In general, partitioning loci encode three elements: centromere-like site(s) in the plasmid DNA, a protein binding to this site and an ATPase. The *Escherichia coli* plasmid R1 *par* locus encodes an actin-like ATPase (7,8). The R1 *par* centromere-like site (*parC*) contains two sets of five 11 bp direct repeats (iterons) separated by a region containing the *par* promoter (9,10). The iterons serve as operator sequences to which ParR binds and represses the promoter (10,11). ParR binds to multiple sites in the *parC* region in a cooperative manner (12). Binding of ParR to *parC* serves to autoregulate expression of the *par* genes as well as to form a nucleoprotein complex for partitioning (9,10). The ParM protein interacts with the ParR/*parC* complex (13) and forms dynamic F-actin-like filaments that are involved in plasmid partitioning (14,15).

In higher eukaryotes, centromere DNA is formed by multifold repeats of satellite DNA. Cloned satellite monomers from many organisms (16–28) exhibit anomalously slow migration in polyacrylamide gels indicative of DNA curvature (29–36). Also human centromeric DNA seems to be curved (26). Curved or bendable DNA aids to the tight winding of the DNA around the histone octamer (37–39).

The bacterial *par* system obviously has centromere and kinetochore function. We thus asked whether the centromeric *parC* DNA of bacteria is also curved and whether it would share the function of DNA curvature and bending in global structure formation of the kinetochore DNA–protein complex in eukaryotes.

Macroscopic DNA curvature has been associated primarily with the presence of properly phased stretches of adenines ['dA_n tracts' (29), for a review see (40)]. Nelson *et al*. (41) crystallized a dA_6 region and solved the structure. Short (4–9 bp) runs of desoxyadenines repeated with the helix screw [$\sim$10.5 bp (42,43)] produce a global curvature of the DNA double helix [(44,45), for reviews see (46–48)]. dA-tract-induced DNA curvature can be affected by other sequence elements (49,50) and also non-dA_n sequence elements can cause DNA curvature (51–54). Curvature is directly related to the Fourier coefficient of the dinucleotide roll angle at a period equal to the helical repeat (55). One of the most accepted hypotheses suggests that distinctive properties of poly(dA):poly(dT) may be explained by having an unusual 'B′-form' structure (32–34) which is sufficiently different from B-form DNA that proteins recognize the difference (56–58). Models of DNA curvature have been proposed (34,36,52,59–63). Numerous examples of naturally occurring DNA curvature have been reported (64–75). Curved DNA has clearly identifiable properties. The curvature measured as retarded gel migration in PAGE is most prominently present at moderate temperatures and decreases at elevated temperatures (31,33,44,76). Ethidium bromide intercalates into the DNA and reduces the differences between B- and B′-form DNA, thereby strongly reducing the migration anomaly (77), in contrast to the behaviour of four-way junctions (78). Wu and Crothers (30) found that a fragment containing the curvature at or near its end migrates most rapidly in

*To whom correspondence should be addressed. Tel: +49 3641 656 260; Fax: +49 3641 656 261; Email: diekmann@imb-jena.de

polyacrylamide gels whereas fragments in which the curvature is more centrally located migrate more slowly.

Here we show that *parC* is indeed curved. We determine the value of the migration anomaly in PAGE and measure its properties. We also compare the curvature of this bacterial centromeric DNA with that of eukaryotic centromeres and discuss the potential influence of curvature on centromere function.

MATERIALS AND METHODS

Those parts of the pKG330 plasmid (Figure 1) relevant for curvature analysis (Figure 2A) were verified by sequencing (MWG, Germany). Approximately 10 µg of pKG330 plasmid DNA carrying the *parC* sequence (see Figure 1) were digested with different restriction endonucleases (New England Biolabs, USA) simultaneously, resulting in different fragments (see Figure 2A) for curvature analysis. According to the time and temperature suggested by the manufacturer (mainly 120 min at 37°C), the DNA was extracted with phenol:chloroform:isoamyl alcohol (15:24:1; Sigma, Germany), precipitated and washed with 80% ethanol, air-dried, re-suspended in 20 µl of 5 mM Tris (pH 8.5) and mixed with 8 µl loading dye solution (60% glycerol, 60 mM EDTA, 0.09% bromphenol blue, 0.09% xylene cyanol FF; MBI Fermentas, Vilnius). The sample (6 µl) was loaded on a native 6% polyacrylamide gel (29:1 acrylamide:bisacrylamide; Bio-Rad, USA). Gels were pre-run for ~3 h until current and temperature remained constant. Unless stated otherwise, electrophoreses was carried out in 1 × TBE (90 mM Tris–borate, 2 mM Na-EDTA, pH 8.0) at 150 V (8 mA) for ~4 h (migration distance of bromphenol blue ~14 cm). The temperature was mainly 24°C (room temperature), or alternatively 4°C (cold room) or 37°C (warm oven). After the runs, the gels were stained for 30 min in an aqueous solution of ethidium bromide (1 mg/l), followed by rinsing in water prior to documentation. The gels were illuminated by a 254 nm UV lamp (Chroma, Brattleboro), documented by a CCD camera system (Polaroid, USA) and gel images printed by a HP Laserjet 2100 M in the size of 26.5 × 18 cm for analysis. The 1 kb plus DNA ladder (Invitrogen, Carlsbad, USA) and the 1 kb DNA ladder (New England Biolabs, USA) served as marker fragments together with the intrinsic plasmid fragments resulting from the restriction digest running in the same lane as the *parC* fragment. For each gel, the migration of all fragments was determined and calibration curves were plotted using the marker fragments (logarithm of the number of base pairs versus distance migrated). The apparent size in the acrylamide gel relative to the calibration curve was determined for every anomaly migrating fragment.

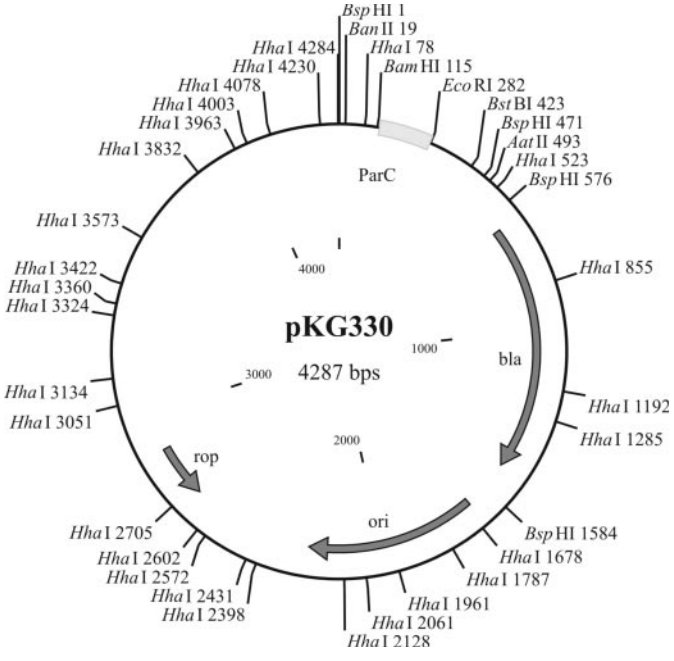

Figure 1. Plasmid pKG330. Restriction sites and the position of *parC* are indicated.

Construction of *parC* H-K mutant sequence

A mutant sequence of the *parC* sequence containing 4 bp exchanges was constructed by DNA cloning procedures using standard methods (79). For the introduction of two new single restriction sites, HindIII and KpnI, between the first (*parC* I) and the second (*parC* II) 5-fold iterons of *parC*, the DNA of plasmid pKG330 was amplified by two PCR reactions (Roche, Penzberg, Germany). In the first reaction, we amplified *parC* I using as upstream primer (*parC* f) 5′-GTAGTAGGTTGAGGCCGTTGAGCAC-3′, which binds ~230 bp upstream of *parC*, and as downstream primer (*parC* Kpn Hind r) 5′-GGTACCCCATTTCAACCATCAATCAAAGCTT-3′, which binds between the two 5-fold iterons and introduces the two new restriction sites. In the second reaction we amplified *parC* II. The upstream primer (*parC* Hind Kpn f) 5′-AAGCTTTGATTGATGGTTGAAATGGGGTACC-3′, a direct antisense repeat of primer (*parC* Kpn Hind r) also introduced the HindIII and KpnI sites, whereas the downstream primer (*parC* Nco r) 5′- CCATGGAAATGTTGAATACTCATACTCTTCC-3′ introduced a NcoI site ~360 bp downstream of *parC*. The blunt end PCR products were cloned into pCR 4Blunt-TOPO (Invitrogen, Carlsbad, CA, USA). The resulting vectors pTOPO*parC* I and pTOPO-*parC* II, carried *parC* I and *parC* II respectively. After verification of the base exchanges by sequencing, both vectors were digested by HindIII–NcoI. The 456 bp fragment of pTOPO*parC* II containing *parC* II was cloned into the 2839 bp fragment of pTOPO*parC* I resulting in pTOPO*parC* H-K. Subsequently pKG330 and pTOPO*parC* H-K were both digested with BamHI–EcoRI. The 167 bp fragment of pTOPO*parC* H-K was cloned into the 4120 bp fragment of pKG330 resulting in pKG330 H-K carrying mutant *parC* with the new restriction sites (*parC* H-K). The exchange of the four bases was confirmed by sequencing (MWG, Ebersbach, Germany). The base pair exchanges are introduced at the sites 192, 194, 219 and 220 bp (see Figure 2). This mutant DNA was digested and analysed as described above for the wild-type sequence.

Computational calculation of curvature

The prediction of DNA curvature was made by means of our **CURVATURE** program. This program calculates a three-dimensional path of a DNA molecule and estimates the curvature of the axis path (80). The CURVATURE algorithm is

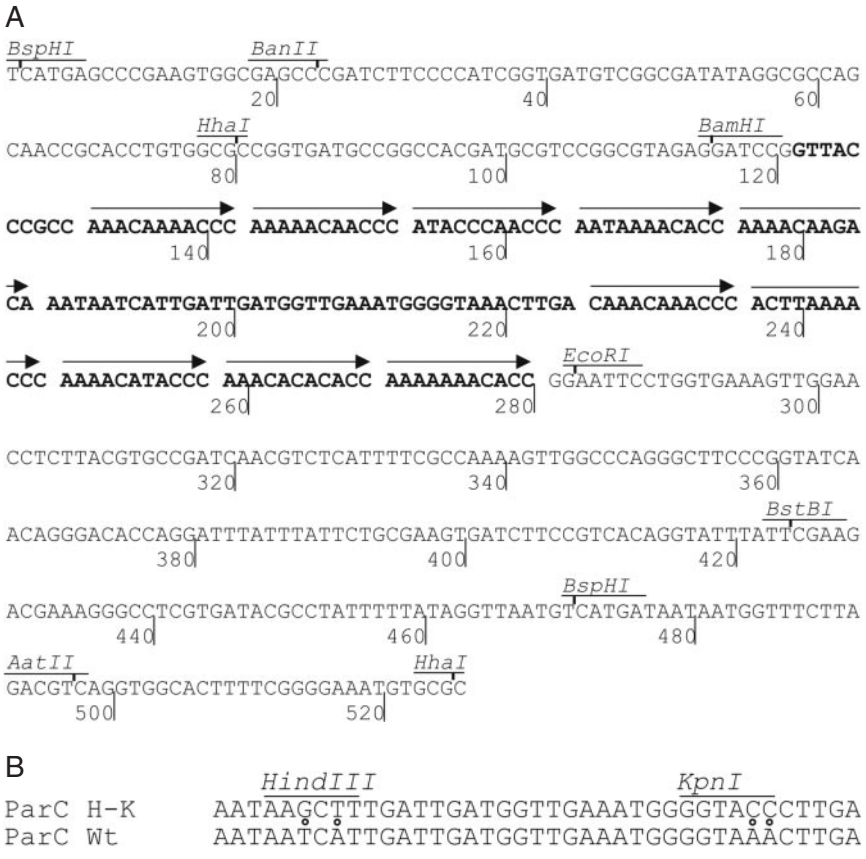

Figure 2. (**A**) The sequence of *parC* (bold, 159 bp) and the framing vector sequences (both verified by sequencing) are displayed. The restriction sites within this DNA are indicated. These restrictions sites were used for fragment analysis. The 11 bp iterons are marked by arrows. (**B**) The mutated *parC* sequence (H-K) and the *parC* wild type (Wt) are displayed. The mutated base pairs are indicated by small circles. The mutations introduce two new single cutting sites HindIII and KpnI.

based on the stepwise calculation of geometric transformations according to the set of dinucleotide wedge angles (52,81). A curvature value at a position *i* corresponds to a curvature of the arc approximating to the predicted DNA path. The DNA curvature was measured in 'DNA curvature units' (cu) introduced by Trifonov and Ulanovsky (82) and in 'degrees per base pair'. Taking 146 bp of DNA wrapping around a histone octamer of 1.65 turns as a basis for conversion, the curvature unit can be related to other measures. For example, having ~88.5 bp in the one full nucleosomal turn we find that 1 cu corresponds to 42.7 degrees per helical turn or ~4.1 degrees per base pair. The program is available upon request from A.B. at bolshoy@research.haifa.ac.il.

RESULTS

The *parC* fragment is 159 bp in length and is organized in two regions each containing a 5-fold repeated sequence motif of 11 bp length with a central region of 39 bp containing the *par* promoter (12). The consensus sequence of the 10 repeats (iterons), dAAAAAAAACCC [(12,83); see Figure 2A], contains longer dA-tracts with a repeat length of 11 bp, thus phased slightly distinct from the DNA helix screw [circa 10.5 bp; (42,43)]. This suggested to us that the *parC* fragment might potentially be curved and thus might show anomalous gel migration. We analysed the *parC* fragment in gels under various conditions.

The *parC* fragment was cloned into the plasmid pKG330 [Figure 1; (83)]. Those parts of the plasmid relevant for curvature analysis were verified by sequencing and are displayed in Figure 2A. Various DNA fragments were constructed by restriction digest using the endonucleases indicated in Figure 2A. These fragments are listed in Table 1. The migration of these fragments relative to a series of marker fragments in different lanes as well as to plasmid fragments in the same lane was analysed in polyacrylamide (6, 8 and 11%) and agarose gels under different buffer and temperature conditions. A typical polyacrylamide gel is displayed in Figure 3. The apparent size of the fragments was determined relative to normally migrating marker fragments. The quotient 'apparent divided by known sequence length' is termed '*k*-factor' [identical to the 'R_L' value (34)] and listed in Table 1 for the different conditions analysed. Several *k*-factor values were measured repeatedly. We deduce an experimental error of the measurements for the *k*-factors of ±0.05.

Most of the plasmid DNA fragments external to the *parC*, migrated normally in the polyacrylamide gels. In particular, those fragments framing the *parC* sequence, migrated normally: SalI/BamHI (276 bp length) upstream and EcoRI/BspHI (189 bp length) downstream had *k*-factors of 0.98 and 1.02, respectively. One fragment, however, which contains the last 120 bp of the origin of replication of the plasmid

Table 1. List of 10 analysed fragments with *k*-factors

Fragment	*k*-factor 8% PAGE; 25°C; 1× TBE Standard		8% PAGE; 1× TBE 4°C		8% PAGE; 1× TBE 50°C		8% PAGE;25°C 0.5 × TBE		8% PAGE; 25°C; 1× TBE 10 mM $MgCl_2$; 170 mM NaCl		25°C; 1× TBE 6% PAGE		25°C; 1× TBE 11% PAGE		8% PAGE; 25°C; 1× TBE EtBr (1 mg/l)		8% PAGE 25°C; 1× TBE EtBr (3 mg/l)		2% Agarose; 1× TBE; 25°C Agarose	
	ParC	ParC H-K	ParC	ParC H-K	ParC	ParC H-K	ParC	ParC H-K	ParC	ParC H-K	ParC	ParC H-K	ParC	ParC H-K	ParC	ParC H-K	ParC	ParC H-K	ParC	ParC H-K
1 120 159 191 BspHI	1.71	1.50	2.45	1.85	1.27	1.21	1.76	1.46	1.68	1.49	1.59	1.38	1.94	1.54			1.00	0.98	1.02	1.02
2 120 159 144 BspHI–BstBI	1.76	1.49	2.30	1.82	1.24	1.19									1.37	1.22			0.99	0.99
3 98 159 217 AatII–BanII	1.68	1.48	2.43	1.78	1.22	1.20	1.69	1.45	1.67	1.48	1.57	1.37	2.07	1.54			1.01	0.97	1.02	1.02
4 41 159 246 HhaI	1.59	1.44	2.03	1.61	1.28	1.21	1.62	1.40	1.66	1.46	1.44	1.29	1.82	1.45			1.01	0.97	1.02	1.02
5 41 159 144 BstBI–HhaI	1.64	1.40	1.91	1.55											1.30	1.13			0.96	0.96
6 6 159 2 BamHI–EcoRI	1.29	1.17	1.53	1.34	1.03	1.0			1.35	1.26		1.20	1.26	1.17	1.08		1.02	0.97	1.02	0.99
7 6 159 144 BamHI–BstBI	1.52		1.89				1.49		1.49		1.34		1.49				1.08			
8 120 159 2 BspHI–EcoRI			1.74				1.35		1.37		1.26		1.30				1.01			
9 270 98 207 TOPO ParC RI SpeI–SnaBI		1.29		1.41				1.23												
10 267 91 213 Topo ParC RII AatII–BsrGI		1.30		1.39				1.28												

The fragments are displayed with the *parC* sequence in grey and the framing plasmid DNA in black. The number of base pairs are printed over the fragment part (length of *parC* is 159 bp). The restrictions sites at the fragment ends are given. Fragments 1 to 6 have *parC* full-size wild-type and mutant sequences. Fragment 9 has the first and 10 has the last 5-fold repeated iteron sequences together with the mutated region between the repeats. Black vertical bars in the *parC* sequences represent the positions of the mutations. The *k*-factors are listed for the various experimental conditions under which they were determined. *ParC* indicates the wild-type, *parC* H-K the mutant sequence. Open table elements indicate that the *k*-factor was not determined for this fragment under these conditions.
For several *k*-factors the mean value of several measurements is given. The error of the *k*-factors is ±0.05.

(HhaI fragment of 270 bp length), migrated slower with a *k*-factor of 1.09 (8% PAGE, 1× TBE, 25°C). Being curved is a property of plasmid replication origins (73) as well as the SV40 origin (75).

The migration anomaly in polyacrylamide gels hardly varies for the salt and buffer conditions analysed here (Table 1). For *parC* framed by 120 and 191 bp on either ends (fragment 1; BspHI digest), at 25°C in 1× TBE (i.e. 90 mM Tris–borate, 2 mM Na-EDTA, pH 8.0) we measured a *k*-factor of 1.71 in 8% PAGE. This changed to 1.76 at 0.5× TBE and 1.68 at physiological conditions (10 mM $MgCl_2$, 170 mM NaCl in the presence of 1× TBE). Other *parC* containing fragments confirmed this invariance (fragments 3, 4 and 7; see Table 1); e.g. for fragment 7 the *k*-factor was 1.52 at 1× TBE, which changed to 1.49 at 0.5× TBE as well as physiological conditions.

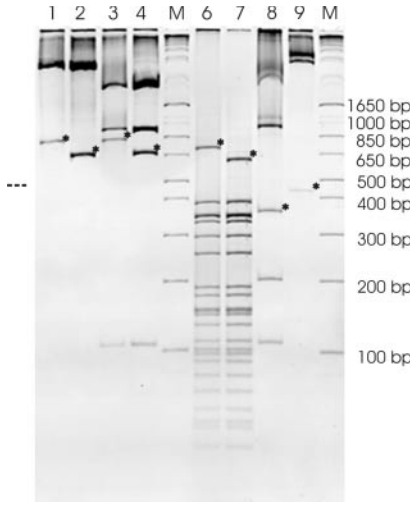

Figure 3. Typical 8% PAGE run with 1× TBE at 25°C. M, marker fragments. Lane 1: fragment 3 (*parC*; AatII/BanII), lane 2: fragment 3 (*parC* H-K; AatII/BanII), lane 3: fragment 1 (*parC*; BspHI), lane 4: fragment 1 (*parC* H-K; BspHI), lane 6: fragment 4 (*parC*; HhaI), lane 7: fragment 4 (*parC* H-K; HhaI), lane 8: fragment 8 (*parC*; BspHI/EcoRI), lane 9: fragment 7 (*parC*; BamHI/BstBI). Numbering of the fragments is according to Table 1. The length of the marker fragments in the two lanes M is given at the right side of the gel. The anomaly migrating fragments containing *parC* are indicated by asterisks. If the anomaly migrating fragments containing *parC* of lanes 1–4 would migrate normally (i.e. according to their sequence length), their position in the gel would be at the site indicated by a broken line at the left side of the gel.

On the other hand, the migration anomaly depends on the polyacrylamide concentration (Table 1). For fragment 1 (BspHI digest) the *k*-factor increased from 1.59 at 6% acrylamide concentration to 1.71 at 8% and 1.94 at 11% (see Figure 4B). Correspondingly, for fragment 4 (HhaI digest) the *k*-factor increased from 1.44 at 6% to 1.59 at 8% and 1.82 at 11% (see Figure 4B). In the measured polyacrylamide concentration range, the *k*-factor increase is linear.

We observed a strong decrease of the migration anomaly with increasing temperature (Table 1). For fragment 1, the *k*-factor decreased from 2.45 at 4°C to 1.71 at 25°C and 1.27 at 50°C (see Figure 4A). For *parC* nearly without framing sequences (6 and 2 bp, BamHI/EcoRI double digest; fragment 6), the *k*-factor decreased from 1.53 at 4°C to 1.29 at 25°C and 1.03 at 50°C (see Figure 4A). Extrapolation suggests that the *k*-factor decreases to 1.00 (normal migration) at a temperature of ∼60–70°C (with a slightly smaller value for fragment 6), as observed for other curved sequences (31,33,44,76).

For controls we measured the migration anomaly of several *parC* containing fragments in agarose gels as well as in the presence of ethidium bromide in the gel buffer. In 2% agarose gels, the migration anomaly of the analysed fragments 1–6 was normal (*k*-factors ∼1.00; see Table 1). In the presence of 1 mg/l ethidium bromide, the migration anomaly was considerably reduced [e.g. for fragment 2 (BspHI/BstBI double digest) the *k*-factor deceased from 1.76 to 1.37]. For most analysed fragments, the migration became normal (*k*-factors ∼1.00; see Table 1) in the presence of 3 mg/l ethidium bromide. This behaviour is known for curved DNA fragments (28,77).

By the exchange of four bases between the two 5-fold repeated iterons within the *parC* sequence (at the sites 192, 194, 219 and 220 bp; see Figure 2A), the *parC* sequence

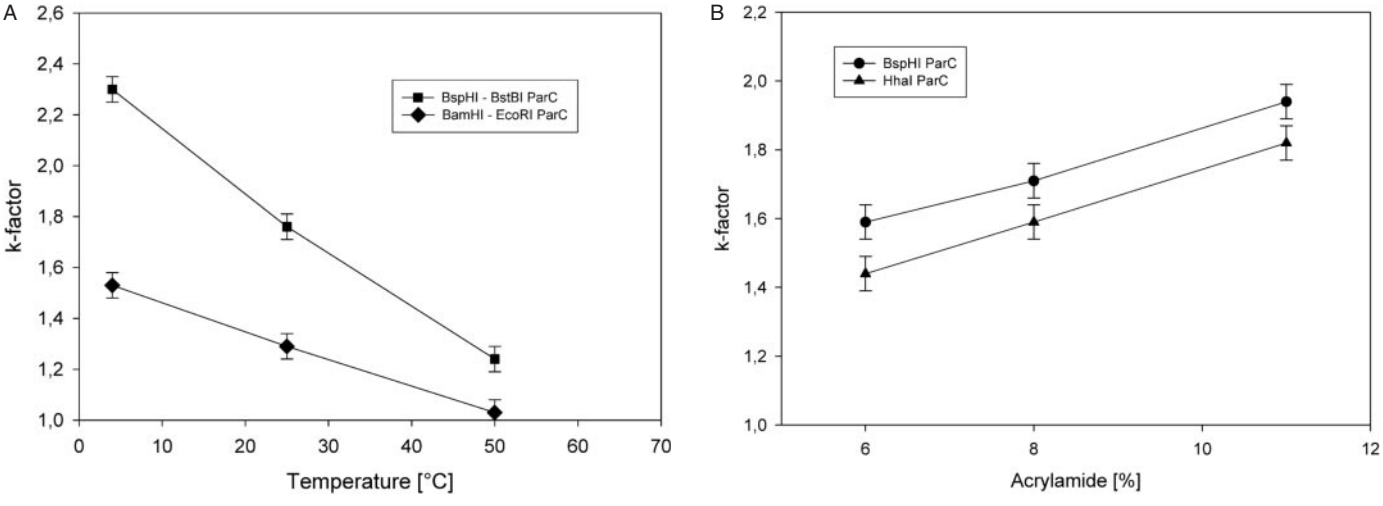

Figure 4. (**A**) Temperature dependence of the *k*-factors of fragments 2 and 6 (see Table 1). Fragment 2 contains framing vector sequences and shows a larger *k*-factor while fragment 6 is *parC*, almost without framing vector sequences. (**B**) Dependence of the *k*-factors of fragments 1 and 4 (see Table 1) on polyacrylamide concentration.

dAATAATCATTGATTGATGGTTGAAATGGGGTAAACTTGA is modified to dAATAAGCTTTGATTGATGGTTGAAATGGGGTACCCTTGA (see Figure 2B) introducing two new single cutting restriction sites. When analysing this modified *parC* sequence, we measured a considerably reduced migration anomaly. For fragment 1 (BspHI digest) the *k*-factor was reduced from 1.71 to 1.50 (same length of DNA; 8% PAGE at 1× TBE at 25°C). A similar reduction was observed for fragments 2–6 (see Table 1). The temperature dependence of the migration anomaly of this modified *parC* sequence was measured to be similar in nature; however, the slope of the *k*-factor versus temperature plot was slightly reduced (data not shown). As for the unmodified *parC* sequence, extrapolation suggests that the *k*-factor decreases to 1.00 (normal migration) at a temperature of ∼60°C for the modified sequence as well. The dependence of the migration anomaly on the polyacrylamide concentration was similar to the unmodified *parC* at 6 and 8% (same slope of *k*-factor versus percentage of acrylamide; data not shown); however, in contrast to the unmodified *parC*, hardly increased further for 11%. Changing the salt and buffer conditions had little or no effect on the migration anomaly (compare fragments 1, 3 and 4 in Table 1), as for the unmodified sequence. In agarose gels as well as in the presence of 3 mg/l ethidium bromide, the modified *parC* migrated normally.

These base pair exchanges create two new single cutting sites within the *parC* sequence, KpnI and HindIII, which allow studying the first and the second 5-fold repeated iterons separately. Using the newly introduced restriction sites, we constructed additional fragments (see Table 1) the migration of which was analysed in gels as well. DNA fragments containing the first 5-fold repeated iteron sequence with framing sequences at the 5′-end only showed rather small migration anomaly. When the up-stream HindIII site was used with framing sequences of 41 (HhaI/HindIII double digest) and 120 bp (BspHI/HindIII double digest) lengths, *k*-factors of 1.10 and 1.04 were measured, respectively (at 1× TBE at 25°C in 8% PAGE; data not shown). In parallel, when the down-stream KpnI site is used with framing sequences of 41 (HhaI/KpnI double digest), 120 (BspHI/KpnI double digest) and 292 bp (SalI/KpnI double digest) lengths, *k*-factors of 1.10, 1.04 and 1.09 were measured, respectively (at 1× TBE at 25°C in 8% PAGE; data not shown). Fragments containing the second 5-fold repeated iteron sequence with framing sequences at the 3′-end only showed larger migration anomaly compared to the fragments containing the first *parC* part, however still small compared to the migration anomaly of the full *parC*. Partly this might be due to the positioning of the curved sequence within the analysed fragment at the 5′ and 3′end, respectively. Maximal migration anomaly is observed when the curved sequence is located in the middle of the fragment (30). When the up-stream HindIII site was used with 3′-framing sequences of 191 (HindIII/BspHI double digest) and 246 bp (HindIII/HhaI double digest) lengths, *k*-factors of 1.15 and 1.19 were measured, respectively (at 1× TBE at 25°C in 8% PAGE; data not shown). In parallel, when the down-stream KpnI site was used with framing sequences of 191 (KpnI/BspHI double digest), 246 (KpnI/HhaI double digest) and 894 bp (KpnI/PstI double digest) lengths, *k*-factors of 1.16, 1.18 and 1.07 were measured, respectively (at 1× TBE at 25°C in 8% PAGE; data not shown).

Using the newly introduced restriction sites, we re-cloned the *parC* 5-fold repeated iterons. We constructed vectors in which either the second or the first part of *parC* was deleted. We thus could analyse fragments in which either the first (fragment 9, SpeI/SnaBI double digest) or the last (fragment 10, AatII/BsrGI double digest, see Table 1) 5-fold repeated iteron sequence was positioned in the middle of the fragment. In 8% PAGE in 1× TBE at 25°C both fragments showed the same migration anomaly which increased to about the same extent at low temperatures (4°C, see Table 1).

Predicted DNA curvature

The software CURVATURE (80) was applied to calculate the trajectories of the wild-type as well as the mutant *parC* sequence. The juxtaposed calculated DNA paths are presented in Figure 5A. The wedge model (36) with the angles of Bolshoy *et al*. (52) and Kabsch *et al*. (81) predicts the planarity of the fragment. Compared to wild type, the modified *parC* sequence displayed a considerably reduced gel mobility. CURVATURE identified changes in the DNA trajectory of the modified *parC* fragment due to the four base exchanges: the modified fragment is less curved than the original *parC* fragment. The two base pair exchanges at 219 and 220 bp result in a curvature reduction at this site of 17 degrees (see Figure 5A). Interestingly, both fragments are rather planar although the iteron repeat length is 11 bp (see Figure 2A), not perfectly matching the helical repeat (10.5 bp). However, the distance between the two sets of iterons (39 bp) is slightly less than an integral number of helical turns so that both effects might compensate. The end-to-end distances for the fragments are 43.9 nm and 39.8 nm, the smaller distance corresponding to the more curved wild-type fragment. The CURVATURE program can be used also to map the DNA curvature along the sequence. In Figure 5B we show the juxtaposed curvature maps of the mutant and wild-type fragments with the window-size of 21 bp. The program predicts that the first pair of modifications (at positions 192 and 194, see Figure 2) should not influence the gel retardation, while the replacement of the dinucleotide dAA by the dinucleotide dCC at positions 219 and 220 (see Figure 2) is predicted to cause a dramatic reduction of the gel migration anomaly.

DISCUSSION

parC is the centromere of the *E.coli* plasmid R1. Here we analysed the intrinsic sequence-directed curvature of *parC* both by its migration anomaly in polyacrylamide gels and by applying the wedge-model based software CURVATURE. The experimentally observed gel migration anomaly indicated as '*k*-factor' (i.e. an apparent fragment length in the gel divided by correct sequence length) of the *parC* sequence is ∼1.7 (see Table 1) and thus smaller than that of another naturally occurring strongly curved DNA, the whole kinetoplast DNA fragment (29,31), which displayed *k*-factors even >4. However, *parC* (159 bp) is much shorter than the kinetoplast fragment (414 bp). When the *parC* curvature is compared with that of parts of the kinetoplast fragment of similar length (e.g. fragments of the lengths 187 and 262 bp) [see (31)], similar *k*-factors were obtained indicating a similar degree of curvature. The *parC* curvature is also similar to that of constructed

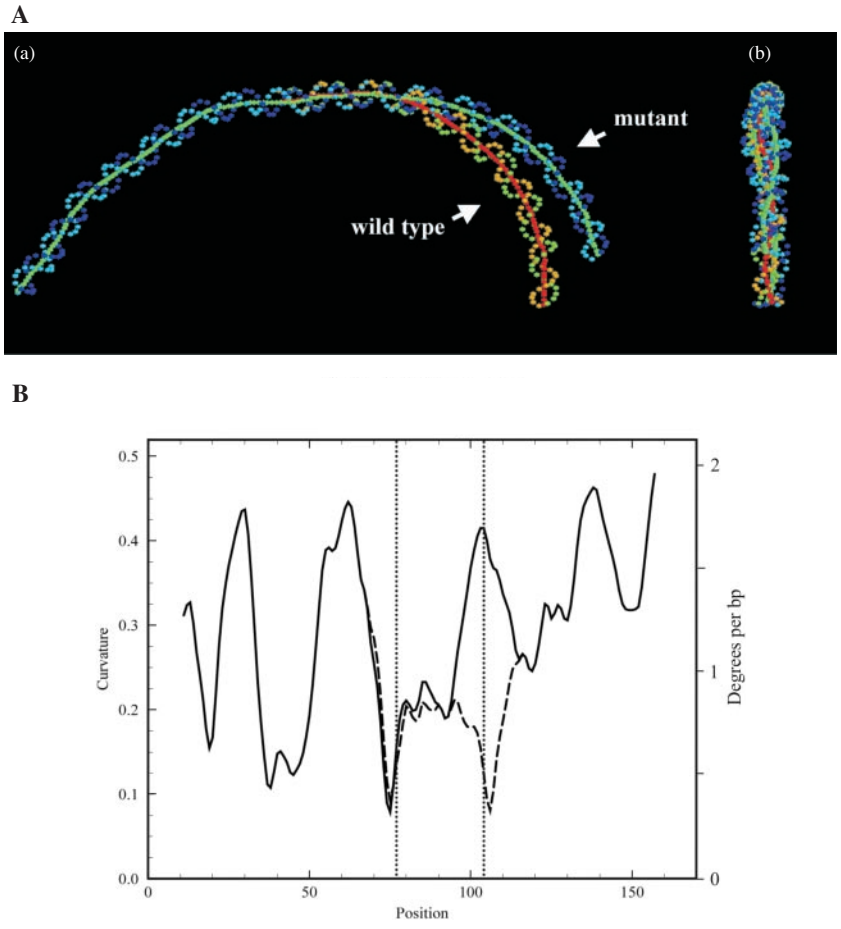

Figure 5. Juxtaposition of predicted DNA curvature for wild-type and modified sequences *parC*. The wild type and modified sequences were applied to the software CURVATURE (80) with the specified parameters (52,81). Both fragments are 167 bp long. The modifications were made at positions 77, 79, 104 and 105 relative to this fragment length (corresponding to sites 192, 194, 219 and 220 in the numbering frame of Figure 2). (**A**) Two-dimensional representation of the DNA paths. Two projections of the DNA paths are presented on a plane of the maximal observed curvature (a) and on a reciprocal plane (b). To display the degree of curvature of a fragment, the calculated coordinates of the phosphates and base pair centers are projected on that plane, for which the mean square distance from all the points is minimal. The line connecting the base pair centers presents the helical axes of the original (wild type: green continued by red) and modified fragment (mutant: green). The phosphates are shown in light and dark blue (mutant) switching to light brown and green for the wild type. The second projection (right) shows the planarity of the fragments. The two base pair exchanges at 219 and 220 bp [resp. 104 and 105 in (B)] result in a curvature reduction at this site of 17 degrees. (**B**) DNA curvature maps versus sequence with window-size of 21 bp. The overall DNA shapes are characterized curvatures of a sliding arc of 21 bp of length approximating to the paths of the axes of the given DNA fragments. The curvature map (given in 'cu units' on the left axis and 'degrees per bp' on the right axis) for wild-type *parC* is plotted as a solid line and for the mutant by a dashed line. The two vertical dotted lines indicate the positions of the base pair modifications.

fragments of similar length with 8-fold repeats of the sequence dGACAAAACTC within framing non-curved sequences (32,33). Thus, for a naturally occurring sequence, the *parC* curvature is large.

The properties of the *parC* curvature agree with those of other curved dA-tract sequences. Just like *parC*, the 187 bp kinetoplast fragment as well as the constructed fragment showed hardly any dependency of the *k*-factor on NaCl or $MgCl_2$ concentration within the measured range (see Table 1) (31,33). Also the temperature dependence [Figure 4A; (84,85)] of the *k*-factors of these DNA fragments is very similar, extrapolating to ~60°C for normal migration (*k*-factor = 1.00) in all three cases (31,33). Furthermore, these fragments behave normally in agarose gels and show a strongly reduced migration anomaly in the presence of ethidium bromide (see Table 1). This similarity in properties of their gel migration anomaly indicates that the phenomenon is of the same origin.

parC contains two regions of 5-fold repeated iterons separated by 39 bp (see Figure 2A). We modified 4 bp within this intermediate sequence creating two new single cutting sites (see Figure 2B). This modified sequence of identical length showed considerably smaller curvature measured in PAGE (see Table 1) and calculated by CURVATURE (see Figure 5A). This indicates that the two repeat regions are not independent curved parts of *parC* but that the overall *parC* curvature is a property of the whole fragment. The intermediate sequence contributes not only by its number of base pairs (which also determines the phasing relation between the first and the second 5-fold repeat) but also to a considerable amount by its sequence.

The two new cutting sites allowed us to analyse the curvature of the first and the second repeat independently. When analysing the first repeat without 3′-framing sequences and the second repeat without 5′-framing sequences, we measured a

smaller curvature for the first repeat. However, when placing the repeats in the centre of fragments with non-curved framing sequences, we found similar *k*-factors for both (Table 1). This discrepancy might be explained by the different arrangement of curved sequences within the repeats, maybe placing curved elements in the first case more to the end of the fragment where their influence on the migration anomaly is reduced (30,31).

Curvature seems to be a general phenomenon of eukaryotic centromeric DNA. Mostly, the degree of curvature is small (*k*-factors of up to 1.20) and only in some cases the *k*-factors are larger (26). All 16 centromere sequences of *Saccharomyces cerevisiae* show migration anomaly in polyacrylamide gels (27,28); the largest *k*-factor value was measured for CEN14 as 1.24. The curvature of most eukaryotic centromere DNA as well as of the 16 yeast sequences is considerably smaller than the curvature of the bacterial centromeric sequence *parC* analysed here.

Since the centromere sequence of an *E.coli* plasmid as well as eukaryotic centromere sequences show DNA curvature, we speculate whether curvature is a general property of centromeres. The centromeres of higher eukaryotes are organised as multi-fold repeats of α-satellite DNA, many of these repeats showing curvature (26). In many eukaryotes, the repeat lengths of the satellite DNA are similar to the repeat lengths of nucleosomes in chromatin or to multimers of this length (26). The satellite curvature might thus serve as a nucleosome positioning signal. Experiments reconstituting nucleosomes onto satellite DNAs confirmed that view (86,87). The curvature of the *parC* sequence found here might support the multiple parR binding to *parC* resulting in a globular folded shape of the kinetochore-like DNA protein complex also in bacteria, may be even similar in size and nature to a nucleosome.

ACKNOWLEDGEMENTS

We thank S. Pfeiffer and S. Hosid for excellent technical support.

REFERENCES

1. Jensen,R.B. and Gerdes,K. (1995) Programmed cell death in bacteria: proteic plasmid stabilization systems. *Mol. Microbiol.*, **17**, 205–210.
2. Gerdes,K., Gultyaev,A.P., Franch,T., Pedersen,K. and Mikkelsen,N.D. (1997) Antisense RNA-regulated programmed cell death. *Annu. Rev. Genet.*, **31**, 1–31.
3. Hiraga,S. (2000) Dynamic localization of bacterial and plasmid chromosomes. *Annu. Rev. Genet.*, **34**, 21–59.
4. Gordon,G.S. and Wright,A. (2000) DNA segregation in bacteria. *Annu. Rev. Microbiol.*, **54**, 681–708.
5. Møller-Jensen,J., Jensen,R.B. and Gerdes,K. (2000) Plasmid and chromosome segregation in prokaryotes. *Trends Microbiol.*, **8**, 313–320.
6. Pogliano,J. (2002) Dynamic cellular location of bacterial plasmids. *Curr. Opin. Microbiol.*, **5**, 586–590.
7. Bork,P., Sander,C. and Valencia,A. (1992) An ATPase domain common to prokaryotic cell cycle proteins, sugar kinases, actin, and heat shock proteins. *Proc. Natl Acad. Sci. USA*, **89**, 7290–7294.
8. Gerdes,K., Møller-Jensen,J. and Jensen,R.B. (2000) Plasmid and chromosome partitioning: surprises from phylogeny. *Mol. Microbiol.*, **37**, 455–466.
9. Dam,M. and Gerdes,K. (1994) Partitioning of plasmid R1. Ten direct repeats flanking the parA promoter constitute a centromere- like partition site *parC*, that expresses incompatibility. *J. Mol. Biol.*, **236**, 1289–1298.
10. Jensen,R.B., Dam,M. and Gerdes,K. (1994) Partitioning of plasmid R1. The parA operon is autoregulated by ParR and its transcription is highly stimulated by a downstream activating element. *J. Mol. Biol.*, **236**, 1299–1309.
11. Breuner,A., Jensen,R.B., Dam,M., Pedersen,S. and Gerdes,K. (1996) The centromere-like parC locus of plasmid R1. *Mol. Microbiol.*, **20**, 581–592.
12. Møller-Jensen,J., Borch,J.Dam,M.Jensen,R.B., Roepstorff,P. and Gerdes,K. (2003) Bacterial mitosis: parM of plasmid R1 moves plasmid DNA by an actin-like insertional polymerization mechanism. *Mol. Cell*, **12**, 1477–1487.
13. Jensen,R.B. and Gerdes,K. (1997) Partitioning of plasmid R1. The ParM protein exhibits ATPase activity and interacts with the centromere-like ParR–parC complex. *J. Mol. Biol.*, **269**, 505–513.
14. Møller-Jensen,J., Jensen,R.B., Lowe,J. and Gerdes,K. (2002) Prokaryotic DNA segregation by an actin-like filament. *EMBO J.*, **21**, 3119–3127.
15. van den Ent,F., Møller-Jensen,J., Amos,L.A., Gerdes,K. and Löwe,J. (2002) F-actin-like filaments formed by plasmid segregation protein ParM. *EMBO J.*, **21**, 1–9.
16. Plohl,M., Borstnik,B., Ugarkovic,D. and Gamulin,V. (1990) Sequence-induced curvature of *Tenebrio molitor* satellite DNA. *Biochimie*, **72**, 665–670.
17. Doshi,P., Kaushal,S., Benyajati,C. and Wu,C.I. (1991) Molecular analysis of the responder satellite DNA in *Drosophila melaogaster*: DNA bending, nucleosome structure and Rsp-binding proteins. *Mol. Evol.*, **8**, 721–741.
18. Barsacchi-Pilone,G., Batistoni,R., Andronico,F., Vitelli,L. and Nardi,I. (1986) Heterochromatic DNA in *Triturus* (Amphibia, Urodela). I. A satellite DNA component of the pericentric C-bands. *Chromosoma*, **93**, 435–446.
19. Kodama,H., Saitoh,H., Tone,M., Kuhara,S., Sakaki,Y. and Mizuno,S. (1987) Nucleotide sequences and unusual electrophoretic behavior of the W chromosome-specific repeating DNA units of the dome fowl, *Gallus gallus domesticus*. *Chromosoma*, **96**, 18–25.
20. Saitoh,Y., Saitoh,H., Ohtomo,K. and Mizuno,S. (1991) Occupancy of the majority of DNA in the chicken W chromosome by bent-repetitive sequences. *Chromosoma*, **101**, 32–40.
21. Radic,M.Z., Lundgren,K. and Hamkalo,B.A. (1987) Curvature of mouse satellite DNA and condensation of heterochromatin. *Cell*, **50**, 1101–1108.
22. Carrera,P., Martinez-Balbas,M.A., Portugal,J. and Azorin,F. (1991) Identification of sequence elements contributing to the intrinsic curvature of the mouse satellite DNA repeat. *Nucleic Acids Res.*, **19**, 5639–5644.
23. Martinez-Balbas,A., Rodriguez-Campos,A., Garcia-Raminez,M., Sainz-Carrera,P., Aymami,J. and Azorin,F. (1990) Satellite DNAs contain sequences that induce curvature. *Biochemistry*, **29**, 2342–2348.
24. Barcelo,F., Gutierrez,F., Barjau,I. and Portugal,J. (1998) A theoretical perusal of the satellite DNA curvature in tenebrionid beetles. *J. Biomol. Struct. Dyn.*, **16**, 41–50.
25. Mestrovic,N., Mravinac,B., Juan,C., Ugarkovic,D. and Plohl,M. (2000) Comparative study of satellite sequences and phylogeny of five species from the genus Palorus (Insecta, Coleoptera). *Genome*, **43**, 776–785.
26. Fitzgerald,D.J., Dryden,G.L., Bronson,E.C., Williams,J.S. and Anderson,J.N. (1994) Conserved patterns of bending in satellite and nucleosome positioning DNA. *J. Biol. Chem.*, **269**, 21303–21314.
27. Ng,R., Ness,J. and Carbon,J. (1986) Structural studies on centromeres in the yeast *Saccharomyces cerevisiae*. *Basic Life Sci.*, **40**, 479–492.
28. Bechert,T., Heck,S., Fleig,U., Diekmann,S. and Hegemann,J.H. (1999) All 16 centromere DNAs of *Saccharomyces cerevisiae* show DNA curvature. *Nucleic Acids Res.*, **27**, 1444–1449.
29. Marini,J.C., Levene,S.D., Crothers,D.M. and Englund,P.T. (1982) Bent helical structure in kinetoplast DNA. *Proc. Natl Acad. Sci. USA*, **79**, 7664–7668.
30. Wu,H.M. and Crothers,D.M. (1984) The locus of sequence-directed and protein-induced DNA bending. *Nature*, **308**, 509–513.
31. Diekmann,S. and Wang,J.C. (1985) On the sequence determinants and flexibility of the kinetoplast DNA fragment with abnormal gel electrophoretic mobilities. *J. Mol. Biol.*, **186**, 1–11.
32. Diekmann,S. (1986) Sequence specificity of curved DNA. *FEBS Lett.*, **195**, 53–56.
33. Diekmann,S. (1987) Temperature and salt dependence of the gel migration anomaly of curved DNA fragments. *Nucleic Acids Res.*, **15**, 247–265.
34. Koo,H.S., Wu,H.M. and Crothers,D.M. (1986) DNA bending at adenine:thymine tracts. *Nature*, **320**, 501–506.

35. Ulanovsky,L., Bodner,M., Trifonov,E.N. and Choder,M. (1986) Curved DNA: design, synthesis, and circularization. *Proc. Natl. Acad. Sci USA*, **83**, 862–866.
36. Ulanovsky,L.E. and Trifonov,E.N. (1987) Estimation of wedge components in curved DNA. *Nature*, **326**, 720–722.
37. Satchwell,S.C., Drew,H.R. and Travers,A.A. (1986) Sequence periodicities in chicken nucleosome core DNA. *J. Mol. Biol.*, **191**, 659–675.
38. Hsieh,C.-H. and Griffith,J.D. (1988) The terminus of SV40 DNA replication and transcription contains a sharp sequence-directed curve. *Cell*, **52**, 535–544.
39. Richmond,T.J. and Davey,C.A. (2003) The structure of DNA in the nucleosome core. *Nature*, **423**, 145–150.
40. Trifonov,E.N. (1985) Curved DNA. *CRC Crit. Rev. Biochem.*, **19**, 89–106.
41. Nelson,H.C., Finch,J.T., Luisi,B.F. and Klug,A. (1987) The structure of an oligo(dA).oligo(dT) tract and its biological implications. *Nature*, **330**, 221–226.
42. Peck,L.J. and Wang,J.C. (1981) Sequence dependence of the helical repeat of DNA in solution. *Nature*, **292**, 375–378.
43. Rhodes,D. and Klug,A. (1981) Sequence-dependent helical periodicity of DNA. *Nature*, **292**, 378–380.
44. Crothers,D.M., Haran,T.E. and Nadeau,J.G. (1990) Intrinsically bent DNA. *J. Biol. Chem.*, **265**, 7093–7096.
45. Diekmann,S. and Travers,A.A. (1992) Formation of B′-DNA structure by homopolymer dA:dT tracts. In Lilley,D.M.J., Heumann,H. and Suck,D. (eds), *Structural Tools for the Analysis of Protein–Nucleic Acid Complexes*. Birkaeuser Verlag, Basel, pp. 63–79.
46. Diekmann,S. (1987) DNA curvature. In Eckstein,F. and Lilley,D.M.J. (eds), *Nucleic Acids and Molecular Biology*. Springer, Berlin, Vol. 1, pp. 138–156.
47. Trifonov,E.N. (1991) DNA in profile. *Trends Biochem. Sci.*, **16**, 467–470.
48. Palecek,E. (1991) Local supercoil-stabilized DNA structures. *Crit. Rev. Biochem. Mol. Biol.*, **26**, 151–226.
49. Haran,T.E., Kahn,J.D. and Crothers,D.M. (1994) Sequence elements responsible for DNA curvature. *J. Mol. Biol.*, **244**, 135–143.
50. Merling,A., Sagaydakova,N. and Haran,T.E. (2003) A-tract polarity dominate the curvature in flanking sequences. *Biochemistry*, **42**, 4978–4984.
51. Bolshoy,A., McNamara,P., Harrington,R.E. and Trifonov,E.N. (1991) Curved DNA without A-A: experimental estimation of all 16 DNA wedge angles. *Proc. Natl Acad. Sci. USA*, **88**, 2312–2316.
52. Brukner,I., Jurukovski,V., Konstantinovic,M. and Savic,A. (1991) Curved DNA without AA/TT dinucleotide step. *Nucleic Acids Res.*, **19**, 3549–3551.
53. Brukner,I., Susic,S., Dlakic,M., Savic,A. and Pongor,S. (1994) Physiological concentration of magnesium ions induces a strong macroscopic curvature in GGGCCC-containing DNA. *J. Mol. Biol.*, **236**, 26–32.
54. Dlakic,M. and Harrington,R.E. (1995) Bending and torsional flexibility of G/C-rich sequences as determined by cyclization assays. *J. Biol. Chem.*, **270**, 29945–29952.
55. Calladine,C.R. and Drew,H.R. (2004) *Understanding DNA*, Academic Press, London.
56. Diekmann,S. and Zarling,D.A. (1987) Unique poly(dA):poly(dT) B′-conformation in cellular and synthetic DNAs. *Nucleic Acids Res.*, **15**, 6063–6074.
57. Zarling,D.A., Diekmann,S. and Calhoun,C.J. (1988) Protein recognition of B′-$(dA)_n$.$(dT)_n$ sequences and kinetoplast DNA. In Olson,W.K., Sarma,M.H., Sarma,R.H. and Sundaralingam,M. (eds), *Structure and Expression*. Adenine Press, Schenectady, NY, Vol. 3, pp. 87–96.
58. Diekmann,S. and McLaughlin,L.W. (1988) DNA curvature in native and modified EcoRI recognition sites and possible influence upon the endonuclease cleavage reaction. *J. Mol. Biol.*, **202**, 823–834.
59. DeSantis,P., Palleschi,A., Savino,M. and Scipioni,A. (1990) Validity of the nearest neighbour approximation in the evaluation of the electrophoretic manifestations of DNA curvature. *Biochemistry*, **29**, 9269–9273.
60. Gorin,A.A., Zhurkin,V.B. and Olson,W.K. (1995) B-DNA twisting correlates with base-pair morphology. *J. Mol. Biol.*, **247**, 34–48.
61. Anselmi,C., DeSantis,P., Paparcone,R., Savino,M. and Scipioni,A. (2002) From the sequence to the superstructural properties of DNAs. *Biophys. Chem.*, **95**, 23–47.
62. Barbic,A., Zimmer,D.P. and Crothers,D.M. (2003) Structural origins of adenine-tract bending. *Proc. Natl Acad. Sci. USA*, **100**, 2369–2373.
63. Beveridge,D.L., Dixit,S.B., Barreiro,G. and Thayer,K.M. (2004) Molecular dynamics simulations of DNA curvature and flexibility: helix phasing and pre-melting. *Biopolymers*, **73**, 380–403.
64. Bossi,L and Smith,D.M. (1984) Conformational Change in the DNA associated with an unusual promoter mutation in a tRNA operon of Salmonella. *Cell*, **39**, 643–652.
65. Wada-Kiyama,Y., Kuwabara,K., Sakuma,Y., Onishi,Y., Trifonov,E.N. and Kiyama,R. (1999) Localization of curved DNA and its association with nucleosome phasing in the promoter region of the human estrogen receptor alpha gene. *FEBS Lett.*, **444**, 117–124.
66. Gabrielian,A.E., Landsman,D. and Bolshoy,A. (1999–2000) Curved DNA in promoter sequences. *In silico Biol.*, **1**, 183–196.
67. Bolshoy,A. and Nevo,E. (2000) Ecologic genomics of DNA: upstream bending in prokaryotic promoters. *Genome Res.*, **10**, 1185–1193.
68. Kaji,M., Matsushita,O., Tamai,E., Miyata,S., Taniguchi,Y., Shimamoto-Katayama,S., Morita,S. and Okabe,A. (2003) A novel type of DNA curvature present in a *Clostridium perfringens* ferredoxin gene: characterization and role in gene expression. *Microbiology*, **149**, 3083–3091.
69. Jauregui,R., Abreu-Goodger,C., Moreno-Hagelsieb,G., Collado-Vides,J. and Merino,E. (2003) Conservation of DNA curvature signals in regulatory regions of prokaryotic genes. *Nucleic Acids Res.*, **31**, 6770–6777.
70. Wanapirak,C., Kato,M., Onishi,Y., Wada-Kiyama,Y. and Kiyama,R. (2003) Evolutionary conservation and functional synergism of curved DNA at the mouse epsilon- and other globin-gene promoters. *J. Mol. Evol.*, **56**, 649–657.
71. Prosseda,G., Falconi,M., Giangrossi,M., Gualerzi,C.O., Micheli,G. and Colonna,B. (2004) The virF promoter in *Shigella*: more than just a curved DNA stretch. *Mol. Microbiol.*, **51**, 523–537.
72. Zahn,K and Blattner,F.R. (1985) Sequence-induced DNA curvature at the bacteriophage lambda origin of replication. *Nature*, **317**, 451–453.
73. Koepsel,R.R. and Khan,S.A. (1986) Static and initiator protein-induced bending of DNA at a replication origin. *Science*, **233**, 1316–1318.
74. Snyder,M., Buchman,A.R. and Davis,R.W. (1986) Bent DNA at a yeast autonomously replicating sequence. *Nature*, **324**, 87–89.
75. Ryder,K., Silver,S., DeLucia,A.L., Fanning,E. and Tegtmeyer,P. (1986) An altered DNA conformation in origin region I is a determinant for the binding of SV40 large T antigen. *Cell*, **44**, 719–725.
76. Ussery,D.W., Higgins,C.F. and Bolshoy,A. (1999) Environmental influences on DNA curvature. *J. Biomol. Struct. Dyn.*, **16**, 811–823.
77. Wu,H.M. (1982) DNA sequence and protein binding induced DNA bending. PhD Thesis. Department of Chemistry, Yale University, New Haven, CT.
78. Diekmann,S. and Lilley,D.M.J. (1987) The anomalous gel migration of a stable cruciform: temperature and salt dependence, and some comparison with curved DNA. *Nucleic Acids Res.*, **15**, 5765–5774.
79. Ausubel,F.M., Brent,R., Kingston,R.E., Moore,D.D., Seidman,J.G., Smith,J.A. and Struhl,K.(eds) (1994) *Current Protocols in Molecular Biology*. John Wiley and Sons, New York.
80. Shpigelman,E.S., Trifonov,E.N. and Bolshoy,A. (1993) CURVATURE: software for the analysis of curved DNA. *Comput. Appl. Biosci.*, **9**, 435–440.
81. Kabsch,W., Sander,C. and Trifonov,E.N. (1982) The 10 helical twist angles of B-DNA. *Nucleic Acids Res.*, **10**, 1097–1104.
82. Trifonov,E.N. and Ulanovsky,L.E. (1987) Inherently curved DNA and its structural elements. In Wells,R.D. and Harvey,S.C. (eds), *Unusual DNA Structures*. Springer-Verlag, Berlin, pp. 173–187.
83. Gerdes,K. and Molin,S. (1986) Partitioning of plasmid R1: structural and functional analysis of the parA locus. *J. Mol. Biol.*, **190**, 269–279.
84. Chan,S.S., Breslauer,K.J., Austin,R.H. and Hogan,M.E. (1993) Thermodynamics and premelting conformational changes of phased $(dA)_5$ tracts. *Biochemistry*, **32**, 11776–11784.
85. Mollegaard,N.E. and Nielsen,P.E. (2003) Increased temperature and 2-methyl-2,4-pentanediol change DNA structure of both curved and uncurved adenine/thymine rich sequences. *Biochemistry*, **42**, 8587–8593.
86. Bock,H., Abler,S., Zhang,X.Y., Fritton,H. and Igo-Kemenes,T. (1984) Positioning of nucleosomes in satellite I-containing chromatin of rat liver. *J. Mol. Biol.*, **176**, 131–154.
87. Linxweiler,W. and Hörz,W. (1985) Reconstitution experiments show that sequence-specific histone DNA interactions are the basis for nucleosome phasing on mouse satellite DNA. *Cell*, **42**, 281–290.